J E M T
Journal of Earth and Marine Technology
homepage URL: ejurnal.itats.ac.id/jemt

Deciphering Metamorphism of Tarap Formation through Petrographic Analysis

Muhammad Alfath Salvano Salni *[1], Idarwati [1]
[1] Department of Mining and Geological Engineering, Universitas Sriwijaya, Jl. Raya Palembang - Prabumulih, KM 32, Indralaya, Kab. Ogan Ilir, Sumatera Selatan 30662, Indonesia
*e-mail: muhammadalfathsalvanosalni@ft.unsri.ac.id

Article info
Received:
May 14, 2026
Revised:
Jul 7, 2026
Accepted:
Jul 16, 2026
Published:
Jul 31, 2026

Keywords:
Tarap Formation; Petrography; Protolith; Metamorphic Facies; OKU Selatan

Abstract
Detailed petrographic characterization aimed at constraining the metamorphic evolution of the Tarap Formation remains limited. This study presents petrographic analyses of 11 metamorphic rock samples collected from the Tarap Formation in OKU Selatan, South Sumatra. The results identify a range of metamorphic rock types, including metalimestone, metasiltstone, calcite–chlorite marble, muscovite–quartz phyllite, quartz–muscovite schist, muscovite–chlorite schist, and quartz–hornblende schist. The protoliths identified were calcareous rocks, quartz–feldspathic sandstones, and shales, which may be lithologically correlated to the Kuantan Formation and Gunungkasih Complex. The metamorphic facies identified are sub-greenschist, greenschist, and lower amphibolite facies. Prograde metamorphism and the subsequent development of mylonitic texture that overprints the main foliation are interpreted to be possibly related to the tectonic evolution of Sumatra during the Early Cretaceous, particularly subduction of the Ngalau Ocean (Meso-Tethys) beneath the Sundaland margin (West Sumatra). The subsequent arc-continent collision from the Late Cretaceous, causing reverse faulting and fold–thrust deformation, facilitated exhumation of the rocks, potentially resulting in retrograde metamorphism and cataclastic texture.

1. Introduction

The Tarap Formation constitutes part of the Garba Mountains, a geologically complex region that records a prolonged history of tectonic activity from the Triassic to Tertiary periods. This region is characterized by a diverse assemblage of pre-Tertiary rocks, including metamorphic rocks, mélange complexes, intrusive and extrusive igneous bodies, and metasedimentary sequences [1], [2], [3], [4]. These lithological associations reflect a complex tectonic evolution associated with subduction, accretion, and subsequent deformation in southern Sumatra.

Stratigraphically, the Tarap Formation represents the oldest lithological unit within the Garba Mountains and forms part of the pre-Tertiary basement complex. The formation is intruded by granitoid rock and unconformably overlain by Paleogene sedimentary units such as the Lahat and Talang Akar Formations, marking the initiation of basin development in South Sumatra [1]. The formation is dominated by metamorphic rocks that are exposed at both the eastern and western margins of the inlier, where they are tectonically imbricated and in thrust contact with the unmetamorphosed Lower Cretaceous Garba Formation. Tarap Formation is interpreted as metamorphosed Paleozoic basement rocks affiliated with the West Sumatra Block [1], [3].

Previous studies have provided initial insights into the deformation and microstructural characteristics of the Tarap Formation. Microstructural analysis by Idarwati et al. (2025) [5] identified evidence of deformation such as changes in mineral orientation and offsets in foliation patterns indicative of shear zone development. Additionally, the presence of metagranite lenses and pinch-outs filling fissures within phyllite. However, research on detailed petrographic characterization aimed at constraining the metamorphic evolution of Tarap Formation remains limited. Even though petrographical assessment has proven effective in constraining the origin and evolutionary history of metamorphic rocks in Indonesia [6], [7], [8]. Therefore, this study aims to decipher the metamorphism of Tarap Formation based on petrographical analysis by identifying rock type, structure, texture, protolith, facies, and their relation to regional tectonic evolution.

2. Methodology

Fieldwork was conducted at OKU Selatan, South Sumatra, where 11 rock samples were collected from outcrops (Figure 1). The samples were subsequently prepared as thin sections. Petrographic analysis was performed using a Euromex iScope Polarizing Microscope at the Petrology Laboratory of Sriwijaya University. The analysis was used to quantify the mineral proportion using a random point counting method with 200 points utilizing Jmicrovision 1.5.3. In addition, textural and structural characteristics were documented.

The petrographic data obtained were interpreted to evaluate rock type, protolith, metamorphic facies, and metamorphic processes. The rock type was determined in accordance with the recommendations of the International Union of Geological Sciences (IUGS) [9]. Protolith interpretation was based on mineral proportions using a ternary diagram of sedimentary protolith metamorphic rock subdivision following Robertson (1999). Metamorphic facies were determined by the occurrence of diagnostic mineral assemblages relative to metamorphic facies mineralogy, following Ehlers & Blatt (1982) [11], Yardley & Warren (2021) [12], and Turner (1968) [13]. Documented textures were used to infer metamorphic processes [14].

3. Results and discussions

3.1. Field observation

Field observations of the Tarap Formation reveal that the formation is composed of various metamorphic rock types, including meta-sedimentary rocks, phyllite, schist, and marble. Meta-sedimentary rocks still preserve relic sedimentary structures, particularly interbedding marked by contrasting whitish meta-limestone and darker metasiltstone layers (Figure 2A), indicating that the original protolith features were not completely obliterated during metamorphism, which is common in low-grade metamorphic rock [16]. Phyllite exhibits well-developed foliation accompanied by microfold structures (Figure 2B), suggesting deformation under compressional stress during metamorphism. Schist shows more prominent and continuous foliation than phyllite (Figure 2C), reflecting stronger mineral alignment and recrystallization [17]. In contrast, marble occurs as a non-foliated metamorphic rock (Figure 2D), consistent with recrystallization dominated by carbonate minerals.

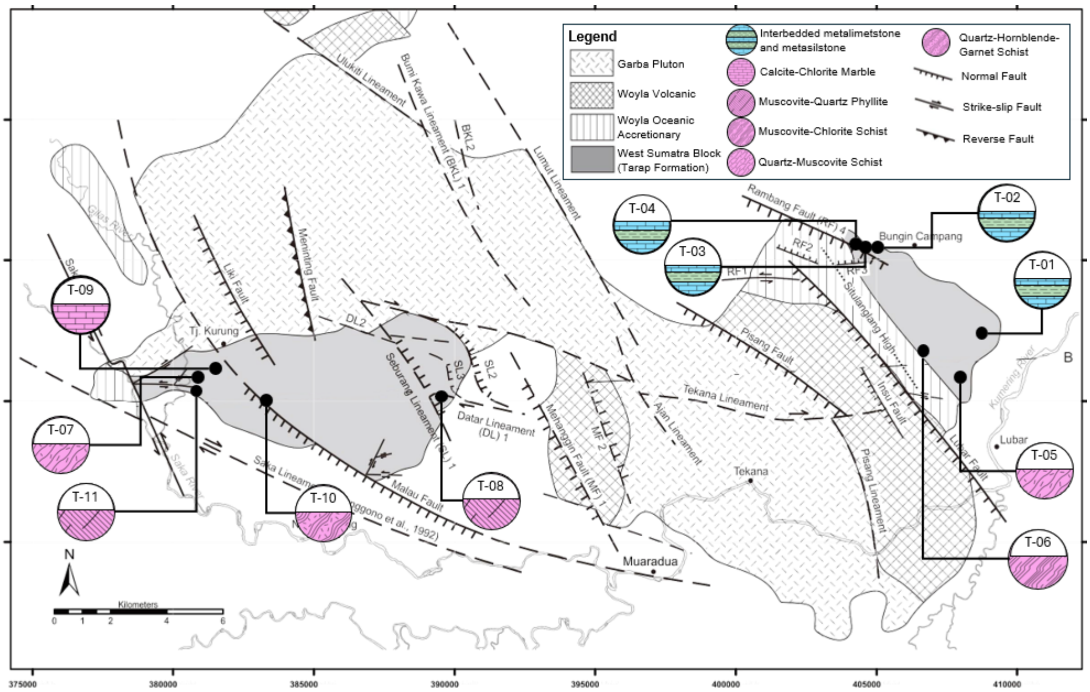

Figure 1. Sample locations overlaid on the geological map of the Garba Mountains modified from Idarwati (2022) [15].

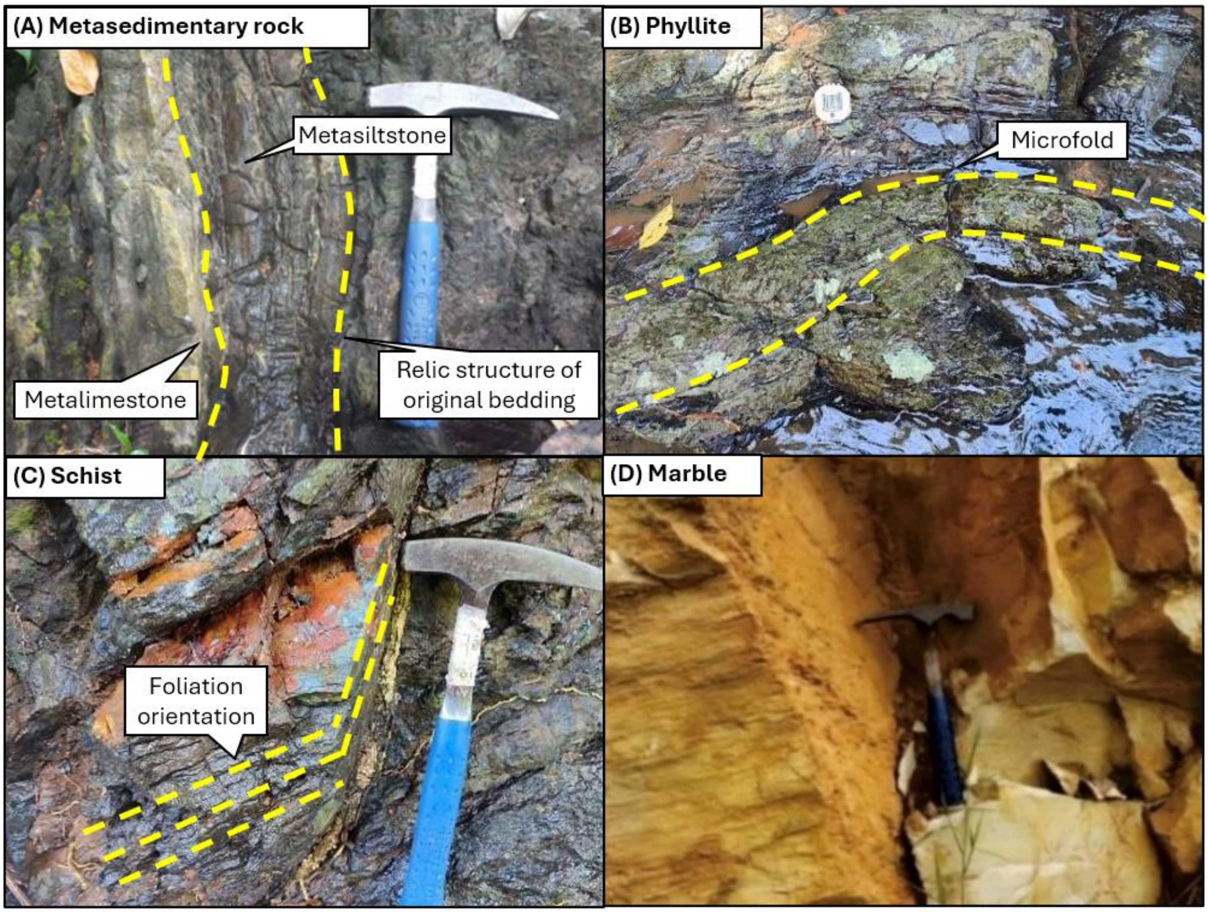

Figure 2. Representative outcrop of (A) meta-sedimentary rock, (B) phyllite, (C) schist and (D) marble.

3.2. Petrographic characteristics

The summary of the petrographic analysis is presented in Table 1. Based on mineral assemblages and textural features, seven metamorphic rock types were identified in the study area. These are broadly classified into non-foliated and foliated groups. The non-foliated rocks consist of metalimestone (Figure 3A-B), metasiltstone (Figure 3B), and calcite–chlorite marble (Figure 3C). Meanwhile, the foliated rocks include muscovite–quartz phyllite (Figure 4A), muscovite–chlorite schist (Figure 4B), quartz–muscovite schist (Figure 4C), and quartz–hornblende schist (Figure 4D).

Various metamorphic structures and textures were identified across the samples studied. Metalimestone is mainly composed of calcite with subordinate quartz. Micrite is mostly preserved, while fossil fragments were no longer observed in the samples examined (Figure 3A). Meanwhile, metasiltstone is dominated by quartz and still preserves clay-rich matrix material (Figure 3B). In contrast, marble shows prominent metamorphic features of saccharoidal texture (Figure 3C), a sugar-like mosaic of interlocking calcite [14].

In foliated rocks, phyllitic and schistose textures are well developed, reflecting preferred mineral alignment [18]. In the muscovite–chlorite schist, a pseudomorphic texture is observed, where chlorite replaces garnet porphyroblasts. The relict garnet contains mineral inclusions, indicating a poikiloblastic texture, with inclusion trails aligned parallel to the external foliation (Figure 4C). The pseudomorphed garnet also forms an augen texture, occurring as lenticular, eye-shaped porphyroblastic relics enclosed within a finer-grained, foliated metamorphic matrix (Figure 4C). The quartz–hornblende schist displays cataclastic deformation of garnet and hornblende (Figure 4D), suggesting brittle deformation. Mylonitic texture is present in both non-foliated (Figure 3B) and foliated rocks (Figure 4B), characterized by fine-grained recrystallized minerals forming a lineated fabric that overprints the primary foliation or fabric (Figure 4B) [14].

Table 1. Mineral proportion and texture that are identified from petrographical analysis.

Code	Mineral proportion (%)											Metamorphic Texture	Rock Nomenclature
	Qz	Pl	Cc	Prh	Act	Grt	Ms	Bt	Chl	Hbl	Op		
T-01	13	4	65	2	-	-	-	-	15	-	1	-	Metalimestone
T-02	47	5	46	-	-	-	-	-	-	-	2	Myl	Metasiltstone
T-03	17	0	73	-	-	-	-	-	8	-	2	-	Metalimestone
T-04	6	3	64	-	-				24		3	-	Metalimestone
T-05	58	6	-	-	-	-	20	-	14	-	2	Sch	Quartz-Muscovite Schist
T-06	6	3	8	-	-	-	20	-	56	-	7	Sch, Ps, Myl, Aug, Pbl, Pkl	Muscovite-Chlorite Schist
T-07	49	7	3	-	-	5	-	17	-	19	-	Sch, Ctc, Pbl	Quartz-Hornblende Schist
T-08	26	8	-	-	-	-	66	-	-	-	-	Phy	Muscovite-Quartz Phyllite
T-09	-	-	94	-	-	-	-	-	6	-	-	Sac	Calcite-Chlorite Marble
T-10	45	4	15	-	11	-	24	-	-	-	1	Sch	Quartz-Muscovite Schist
T-11	32	5	-	-	-	-	63	-	-	-	-	Phy	Muscovite-Quartz Phyllite

Mineral abbreviation
Qz = Quartz, Pl = Plagioclase, Cc = Calcite, Prh = Prehnite, Act = Actinolite, Grt = Garnet, Ms = Muscovite, Bt = Biotite, Chl = Chlorite, Hbl = Hornblende, Op = Opaque mineral

Texture abbreviation
Myl = Mylonitic, Sch = Schistose, Ps = Pseudomorph, Aug = Augen texture, Ctc = Cataclastic, Phy = Phyllitic, Sac = Saccaroidal, Pkl = Poikiloblastic, Pbl = Porphyroblastic

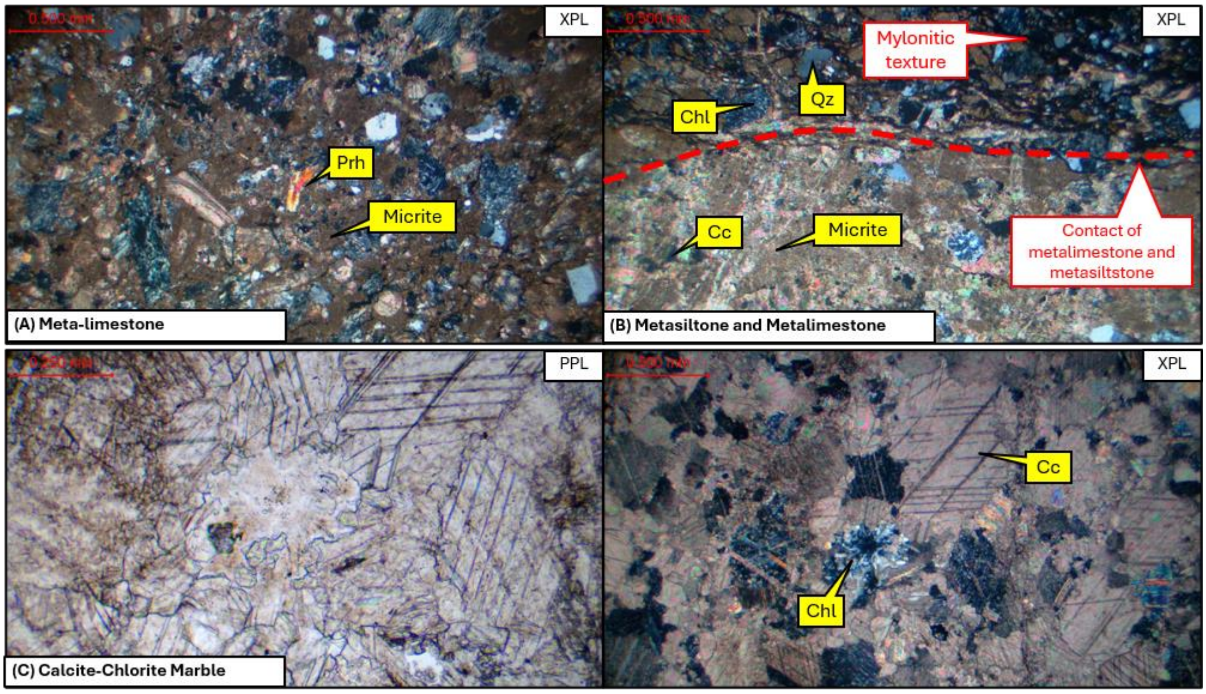

Figure 3. Microphotographs of (A) Metalimestone, (B) Interbedding of metasiltstone and metalimestone, and (C) Calcite-chlorite marble.

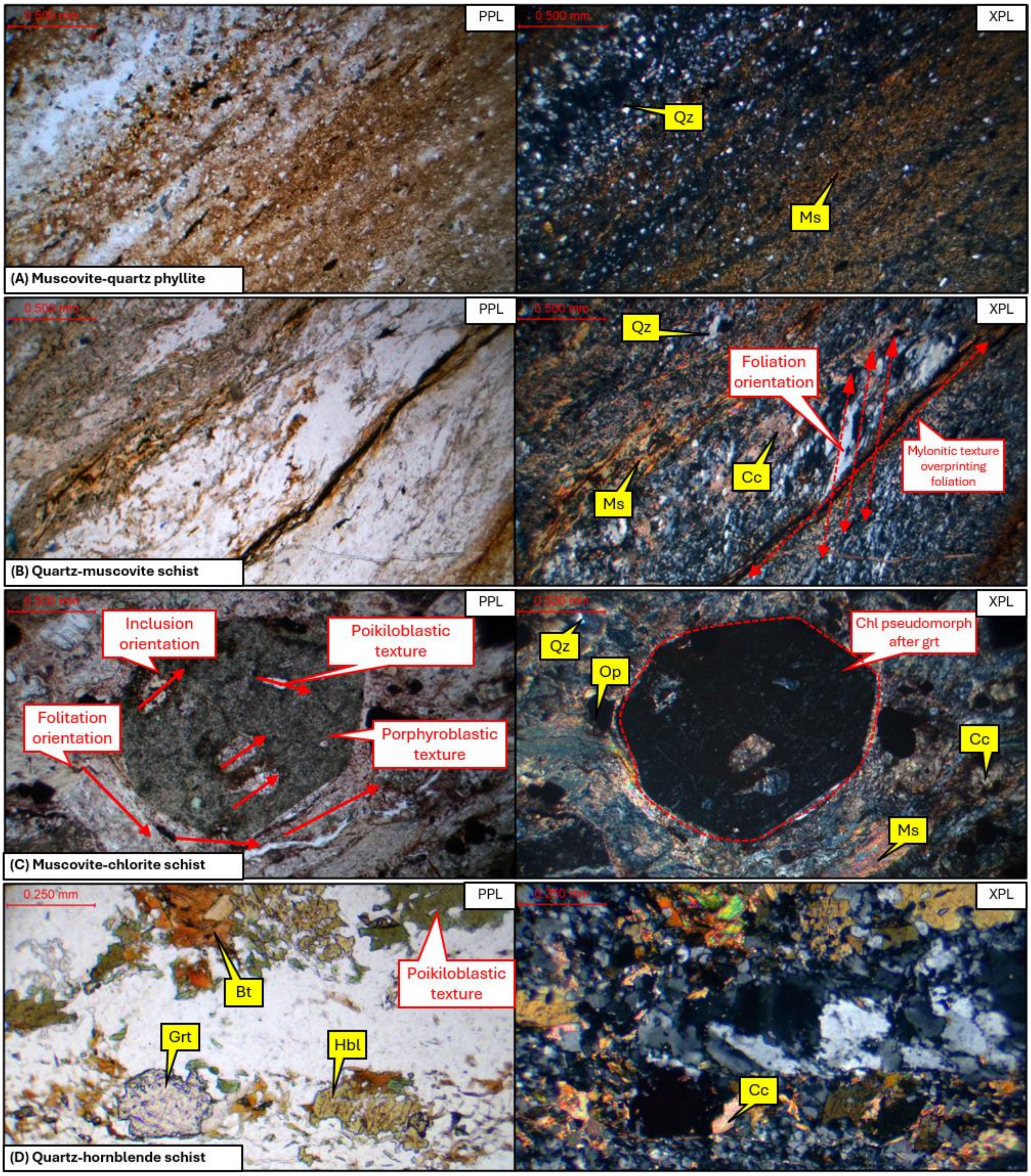

Figure 4. Microphotograph of (A) Muscovite-quartz phyllite, (B) Quartz-muscovite schist, (C) Muscovite-chlorite schist and (D) Quartz-hornblende schist.

3.3. Protolith

Protolith determination was carried out based on mineral proportions using metamorphic rock subdivision ternary diagrams adapted from Robertson (1999) [10] (Figure 5). The absence of mafic minerals in all samples indicates that mafic protoliths are unlikely. The identified protoliths include limestone (metacarbonate rock), calcareous sandstone (calcareous psammite), quartz-feldsphatic sandstone (psammite), siltstone (semipelite) and shale (pelite).

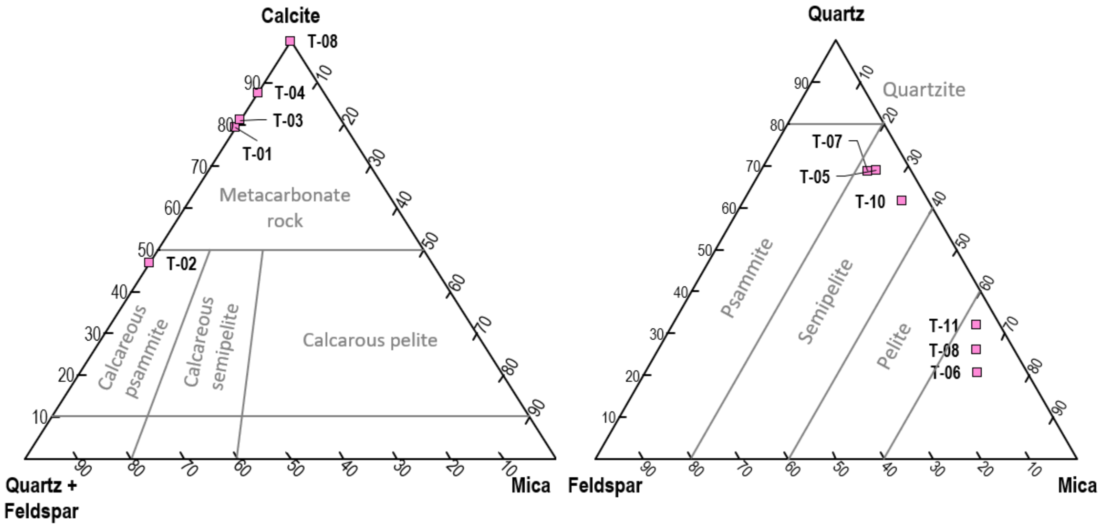

Figure 5. Ternary diagram of sedimentary protolith-based classification of metamorphic rock (modified from Robertson (1999) [10]).

The lithological characteristics and inferred protoliths of the Tarap Formation are broadly comparable to those of the Gunungkasih Complex in Lampung [19]. Both units include interpreted pelitic rocks and quartz–feldspathic sandstones as protoliths, although the Gunungkasih Complex also contains mafic protoliths that were not identified in the Tarap Formation [20]. Likewise, the inferred protolith assemblage of the Tarap Formation resembles that of the Kuantan Formation, which forms part of the basement of the West Sumatra Block and is composed predominantly of turbiditic sandstones and shales with minor limestone [19]. These similarities are based primarily on lithological and petrographic observations**.** Nevertheless, they are consistent with the hypothesis proposed by Gafoer et al. (1993) [1] that suggested that the Tarap Formation may represent metamorphosed Paleozoic basement rocks of the West Sumatra Block.

3.4. Metamorphic facies

Three metamorphic facies are identified, namely, sub-greenschist, greenschist, and lower amphibolite, based on their mineral assemblages. The sub-greenschist facies is represented by the assemblage of chlorite, calcite, and prehnite. The greenschist facies is characterized by chlorite, muscovite, and actinolite, whereas the lower amphibolite facies is distinguished by the presence of biotite, hornblende and garnet. Comparison with the correlated unit of the Gunungkasih Complex indicates a similar metamorphic progression from greenschist to amphibolite facies [20]. Accordingly, the metamorphic facies can be used to infer range of pressure–temperature conditions, approximately ~100–200 °C and 2–6 kbar for sub-greenschist facies, ~300–500 °C and 2–10 kbar for the greenschist facies, and ~500–700 °C and 2–10 kbar for the lower amphibolite facies (Figure 6) [21], [22]. Summary of rock classification, protolith, and facies are presented in Table 2.

Table 2. Summary of interpreted rock classification, protolith and metamorphic facies

Sample	Rock unit	Protolith	Metamorphic facies
T-01	Metalimestone	Metacarbonate rock (Limestone)	Sub-greenschist facies
T-02	Metasiltstone	Calcareous psamite (Calcareous sandstone)	Sub-greenschist facies
T-03	Metalimestone	Metacarbonate rock (Limestone)	Sub-greenschist facies
T-04	Metalimestone	Metacarbonate rock (Limestone)	Sub-greenschist facies
T-05	Quartz-Muscovite Schist	Semipelite (Siltstone)	Greenschist facies
T-06	Muscovite-Chlorite Schist	Pelite (Shale)	Greenschist facies
T-07	Quartz-Hornblende Schist	Semipelite (Siltstone)	Lower amphibolite facies
T-08	Muscovite-Quartz Phyllite	Pelite (Shale)	Greenschist facies
T-09	Calcite-Chlorite Marble	Metacarbonate rock (Limestone)	Greenschist facies
T-10	Quartz-Muscovite Schist	Semipelite (Siltstone)	Greenschist facies
T-11	Muscovite-Quartz Phyllite	Pelite (Shale)	Greenschist facies

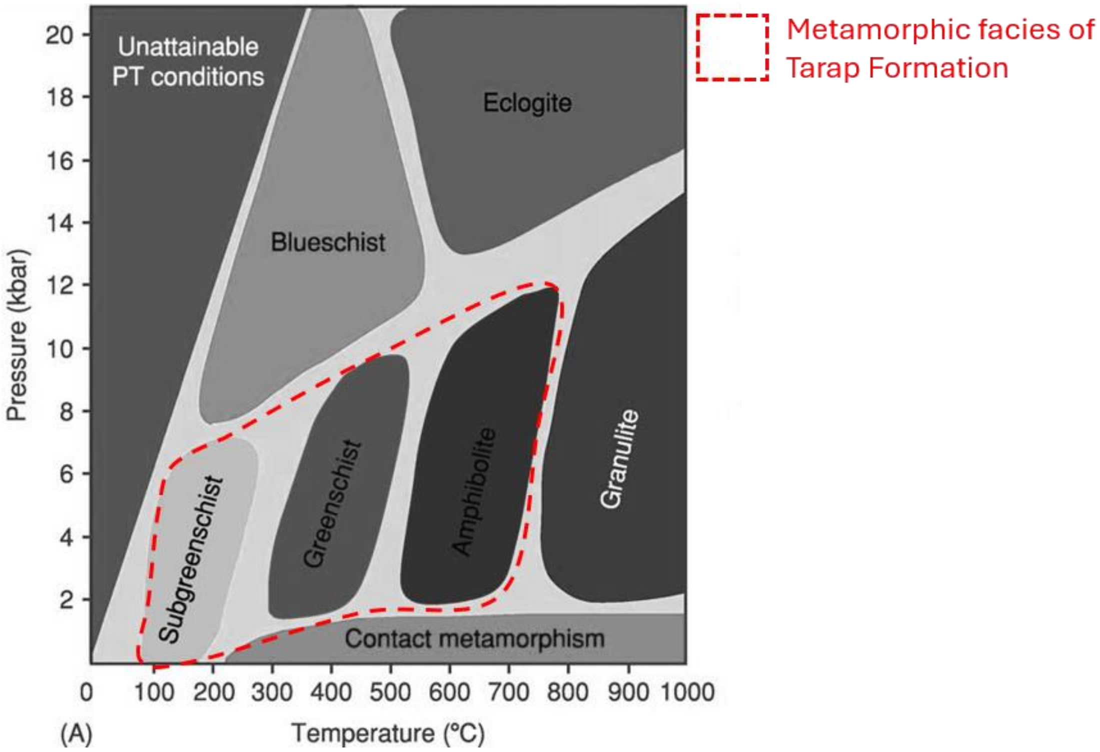

Figure 6. Pressure-Temperature diagram showing metamorphic facies of Tarap Formation. (modified from Butcher (2005) [22])

3.5. Implications for the metamorphism of Tarap Formation

Spatially, Tarap Formation exhibits an increase in metamorphic grade from east to west, as indicated by both texture and mineral assemblages. The eastern sector is dominated by non-foliated meta-sedimentary rock associated with prehnite–pumpellyite facies, which progressively transitions westward into phyllite and schist characterized by greenschist to amphibolite facies. This systematic increase in metamorphic facies, coupled with the development of foliation, is consistent with regional metamorphism that is related to subduction tectonic settings [23]. In addition, the metamorphic facies likely correspond to either Barrovian- or Buchan-type metamorphism. The absence of key index minerals, such as andalusite and kyanite, precludes definitive series determination. Nevertheless, both series are commonly associated with a subduction-related origin [24], [25]. The process is possibly associated with Early Cretaceous subduction of West Sumatra (Margin of Sundaland) and Ngalau Ocean (Meso-Tethys) proposed by Barber et al. (2005) (Figure 7A) [3].

Based on petrographical observation, prograde metamorphism occurred, as it is indicated by the presence of garnet porphyroblasts containing inclusions of finer-grained minerals. The curved inclusion trails following external foliation alignment suggest syn-tectonic growth, implying that garnet crystallized contemporaneously with deformation during progressive pressure increase and heating [26]. The occurrence of mylonitic textures indicates a phase of high-strain ductile deformation [27]. This overprinting relationship of mylonite and foliation suggests that the ductile deformation occurred after the main foliation-forming event, as it is found across metamorphic facies.

The subsequent stage is characterized by retrograde metamorphism and post-peak facies deformation. This is evidenced by the replacement of garnet by lower-grade chlorite forming pseudomorphs, as well as the presence of cataclastically deformed garnet and hornblende. This retrograde overprint may be related to the regional tectonic evolution following arc–continent collision and the emplacement of the Woyla Group suggested by Barber et al. (2005) (Figure 7B). The collision events during the Late Cretaceous to Early Tertiary, including reverse faulting and fold–thrust deformation, played a significant role in modifying the metamorphic assemblages. Continued tectonic activity led to uplift and exhumation of the rocks, associated with the development of an accretionary wedge exposing metamorphic rock to lower temperature and pressure [28]. Similar retrograde metamorphism following arc–continent collision has been documented in other places, such as the Trans-Hudson orogeny and the South Tian Shan [29], [30]. Additionally, faulting processes likely induced cataclastic deformation, which typically occurs under relatively lower pressure and temperature, corresponding to the brittle upper crust during post-collisional tectonics [31].

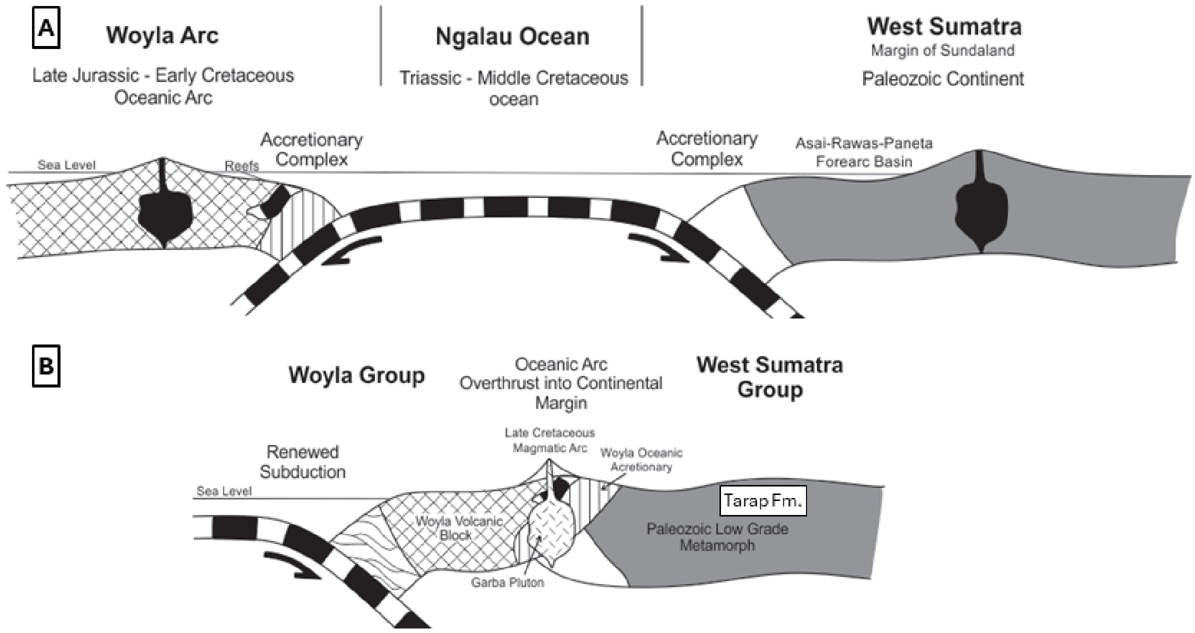

Figure 7. Schematic of (A) Late Jurassic – Early Cretaceous subduction of Ngalau Ocean toward Woyla Arc and West Sumatra and (B) Late Cretaceous Arc-Continent Collision of Woyla Group and West Sumatra Group (modified from Barber et al., 2005 [32]).

4. Conclusion

Petrographic analysis of the Tarap Formation identifies a range of metamorphic rock types, including metasiltstone, metalimestone, calcite–chlorite marble, muscovite–quartz phyllite, quartz–muscovite schist, muscovite–chlorite schist, and quartz–hornblende schist, with protoliths interpreted as calcareous sandstone, limestone, quartz–feldspathic sandstones, siltstone and shale, which possibly correlated to Gunungkasih Complex and the unmetamorphosed equivalents of the Kuantan Formation. Metamorphism reached sub-greenschist, greenschist, and lower amphibolite facies. Prograde metamorphism and mylonitic texture that overprint the main foliation are probably associated with the evolution of Sumatra tectonics during the Early Cretaceous, involving subduction of the Ngalau Ocean (Meso-Tethys) toward West Sumatra (Margin of Sundaland) and the subsequent arc–continent collision. The collisional tectonics from the Late Cretaceous to Early Tertiary, including reverse faulting and fold–thrust development, likely facilitated exhumation, resulting in retrograde metamorphism and cataclastic deformation.

Acknowledgment

The authors would like to express their sincere gratitude to the Petrology Laboratory, Faculty of Engineering, Universitas Sriwijaya, for providing the facilities and technical support necessary to carry out this study.

References

[1] S. Gafoer, T. C. Amin, and R. Pardede, “Geological Map of Baturaja Quadrangle, Sumatra,” Bandung, 1993.

[2] A. J. Barber and M. J. Crow, “An evaluation of plate tectonic models for the development of Sumatra,” *Gondwana Research*, vol. 6, no. 1, pp. 1–28, 2003.

[3] A. J. Barber, M. J. Crow, and M. E. M. De Smet, “Chapter 14 Tectonic Evolution,” in *Sumatra: Geology, Resources and Tectonic Evolution*, vol. 31, no. 1, A. J. Barber, M. J. Milsom, and J. S.

Crow, Eds., Geological Society of London, 2005, pp. 234–259. doi: 10.1144/GSL.MEM.2005.031.01.14.
[4] Idarwati, H. S. Purwanto, E. Sutriyono, and C. Prasetyadi, "Revealing granitic basement of Garba Hill, Muara Dua Region, South Sumatera based on landsat images, structure, and petrography," *IOP Conf. Ser. Earth Environ. Sci.*, vol. 212, p. 012041, Dec. 2018, doi: 10.1088/1755-1315/212/1/012041.
[5] Idarwati, B. Setiawan, S. N. Jati, Y. Z. Rochmana, E. D. Mayasari, and M. Rendana, "Schematic formation of boudine granite and microfold phyllite of Gilas River: Implications for Triassic to Tertiary tectonics of Garba Hill, South Ogan Komering Ulu Regency, South Sumatra Province," *Geosystems and Geoenvironment*, vol. 4, no. 3, p. 100414, Aug. 2025, doi: 10.1016/j.geogeo.2025.100414.
[6] H. Hasria, A. Idrus, and I. Wayan Warmada, "Protolit Batuan Metamorf di Pegunungan Rumbia Kabupaten Bombana, Provinsi Sulawesi Tenggara, Indonesia," *Jurnal Geologi dan Sumberdaya Mineral*, vol. 23, no. 1, pp. 25–33, Feb. 2022, doi: 10.33332/jgsm.geologi.v23i1.638.
[7] N. I. Setiawan *et al.*, "Peak Metamorphic Conditions of Garnet Amphibolite from Luk Ulo Complex, Central Java, Indonesia: Implications for Medium-Pressure/High-Temperature Metamorphism in the Central Indonesian Accretionary Collision Complex," *Indonesian Journal on Geoscience*, vol. 7, no. 3, pp. 225–239, Sep. 2020, doi: 10.17014/ijog.7.3.225-239.
[8] R. Ikhram, I. Syafri, and M. F. Rosana, "Petrology, Geochemistry and K-Ar Dating of Metamorphic Rock in Ciletuh Mélange Complex, West Java Indonesia," *Riset Geologi dan Pertambangan*, vol. 33, no. 1, Jun. 2023, doi: 10.55981/risetgeotam.2023.1054.
[9] R. Schmid *et al.*, "How to Name A Metamorphic Rock," D. Fettes and J. Desmons, Eds., 2011.
[10] S. Robertson, "BGS Rock Classification Scheme Volume 2 Classification of metamorphic rocks," 1999.
[11] E. G. Ehlers and H. Blatt, "Petrology: Igneous, Sedimentary and Metamorphic," 1982. [Online]. Available: https://api.semanticscholar.org/CorpusID:140700948
[12] B. Yardley and C. Warren, *An Introduction to Metamorphic Petrology*, 2nd ed. Cambridge: Cambridge University Press, 2021. doi: DOI: 10.1017/9781108659550.
[13] F. J. Turner, "Metamorphic Petrology; Mineralogical and Field Aspects," 1968. [Online]. Available: https://api.semanticscholar.org/CorpusID:129631427
[14] S. Song and Y. Cao, "Textures and structures of metamorphic rocks," *Encyclopedia of Geology*, vol. 1, p. 6, 2021.
[15] Idarwati, "Evolusi Tektonik Batuan Dasar Bukit Garba Sumatera Selatan," Universitas Pembangunan Nasional "Veteran" Yogyakarta, 2022.
[16] B. P. J. Stevens and G. M. Bradley, "Sedimentology in metamorphic rocks, the Willyama Supergroup, Broken Hill, Australia," *Australian Journal of Earth Sciences*, vol. 65, no. 1, pp. 25–59, Jan. 2018, doi: 10.1080/08120099.2018.1399462.
[17] A. R. Philpotts and J. J. Ague, *Principles of Igneous and Metamorphic Petrology*, 3rd ed. Cambridge: Cambridge University Press, 2022. doi: DOI: 10.1017/9781108631419.
[18] B. R. Frost and C. D. Frost, *Essentials of igneous and metamorphic petrology*. Cambridge University Press, 2019.
[19] A. J. Barber and M. J. Crow, "Chapter 13 Structure and structural history," *Geological Society, London, Memoirs*, vol. 31, no. 1, pp. 175–233, Jan. 2005, doi: 10.1144/GSL.MEM.2005.031.01.13.
[20] H. C. N. Sirait and V. Dewinta, "Petrology and Mineralogy of Metamorphic Rocks in The Pringsewu District, Lampung Province, Indonesia," *Journal of Geoscience, Engineering, Environment, and Technology*, vol. 8, no. 3, pp. 203–211, Aug. 2023, doi: 10.25299/jgeet.2023.8.3.11347.
[21] P. Eskola, "On the relations between the chemical and mineralogical composition in the metamorphic rocks of the Orijarvi region," *Bulletin de la Commission géologique de Finlande*, vol. 44, pp. 109–145, 1915.

[22] K. Bucher, “METAMORPHIC ROCKS | Facies and Zones,” in *Encyclopedia of Geology*, Elsevier, 2005, pp. 402–409. doi: 10.1016/B0-12-369396-9/00319-1.

[23] M. Brown, “The contribution of metamorphic petrology to understanding lithosphere evolution and geodynamics,” *Geoscience Frontiers*, vol. 5, no. 4, pp. 553–569, Jul. 2014, doi: 10.1016/j.gsf.2014.02.005.

[24] Y.-F. Zheng, “Metamorphism in Subduction Zones,” in *Encyclopedia of Geology*, Elsevier, 2021, pp. 612–622. doi: 10.1016/B978-0-08-102908-4.00020-5.

[25] Y.-F. Zheng and R.-X. Chen, “Extreme metamorphism and metamorphic facies series at convergent plate boundaries: Implications for supercontinent dynamics,” *Geosphere*, vol. 17, no. 6, pp. 1647–1685, Dec. 2021, doi: 10.1130/GES02334.1.

[26] P. A. Camilleri, “Classification, character, and origin of textural zoning in porphyroblasts: significance and relation to strain,” *Journal of the Tennessee Academy of Science*, vol. 93, no. 1, p. 0, 2018.

[27] F. Giuntoli, L. Menegon, C. J. Warren, J. Darling, and M. W. Anderson, “Protracted Shearing at Midcrustal Conditions During Large-Scale Thrusting in the Scandinavian Caledonides,” *Tectonics*, vol. 39, no. 9, Sep. 2020, doi: 10.1029/2020TC006267.

[28] S. A. Mangga, T. Amiruddin, T. Suwarti, S. Gafoer, Sidarto, and A. Andra, “Geology of the Tanjungkarang Quadrangle, Sumatra,” 1994.

[29] I. W. Hillenbrand *et al.*, “Paleoproterozoic Reworking of Archean Crust and Extreme Back-Arc Metamorphism in the Enigmatic Southern Trans-Hudson Orogen,” *Geophys. Res. Lett.*, vol. 51, no. 4, Feb. 2024, doi: 10.1029/2023GL107552.

[30] J. R. Worthington *et al.*, “Birth, life, and demise of the Andean–syn-collisional Gissar arc: Late Paleozoic tectono-magmatic-metamorphic evolution of the southwestern Tian Shan, Tajikistan,” *Tectonics*, vol. 36, no. 10, pp. 1861–1912, Oct. 2017, doi: 10.1002/2016TC004285.

[31] I. K. A. Erler, “Pyrite Deformation Textures in the Deposits of the Küre Mining District (Kastamonu-Turkey),” *Turkish Journal of Earth Sciences*, vol. 11, pp. 205–215, 2002, [Online]. Available: https://api.semanticscholar.org/CorpusID:55866546

[32] A. J. Barber, M. J. Crow, and M. E. M. De Smet, “Chapter 14 Tectonic Evolution,” *Geological Society, London, Memoirs*, vol. 31, no. 1, pp. 234–259, Jan. 2005, doi: 10.1144/GSL.MEM.2005.031.01.14.